

GPS-Synchronization of a Seismic Accelerometer and a Ground-Based Interferometric Radar for Structural Health Monitoring

ANDREA CIONCOLINI, LAPO MICCINESI,
ALESSANDRA BENI, LORENZO PAGNINI,
JINGFENG SHAN and MASSIMILIANO PIERACCINI

ABSTRACT

This paper presents a seismic accelerometer with GPS-synchronization based on the pulse per second (PPS) signal provided by the GNSS satellite network. This feature is essential for a Structural Health Monitoring (SHM) network that includes different sensors as for example accelerometers, cameras and a ground-based radar. The PPS signal is widely used in applications of timing synchronization because of its high accuracy and long-term stability. The common time-base between devices allows the internal time of the devices to be resynchronized every second, avoiding drift. In this work, we developed and tested acquisition board for seismic accelerometer with custom firmware designed to provide synchronized data recorded by different acquisition systems. The universal time (UTC) synchronized with PPS has been assigned to the data of each devices. The developed board has been tested with simultaneous acquisition a seismic accelerometer in MEMS (Micro Electro-Mechanical System) technology and a ground-based interferometric radar, both GPS synchronized. The two sensors are equipped with high precision GNSS receiver u-blox F9, that provide the UTC data and the PPS signal. To validate the synchronization system, the accelerometer and the ground-based radar were operated simultaneously to detect the oscillations of a moving target (a metallic swinging rod). The results of the experiment demonstrate that the sensors are well synchronized and the evaluations of the displacement are very similar, with good accuracy for performing dynamic structure monitoring. It is worth noting that this comparative analysis has highlighted the role of the automatic synchronization.

INTRODUCTION

In the field of Structural Health Monitoring (SHM), many heterogeneous sensing systems are used, such as accelerometers [1], interferometric radars [2], and imaging devices [3]. Combining multiple sensors enables more accurate and reliable structural monitoring. This approach offers a clearer state of the building's or bridge's condition. Accurate time synchronization ensures effective data fusion and reliable correlation with external events [4] [5]. The time alignment among various sources is particularly crucial in dynamic scenarios, such as monitoring the effects of traffic loads on bridges or capturing transient oscillations caused by seismic activity. Indeed, a common challenge in multi-sensor SHM networks is clock drift among devices, which can introduce significant temporal mismatches and compromise the integrity of data analysis. To address this, the authors in [6] propose to integrate a high-resolution digital accelerometer with an intelligent wireless sensor (WSS) platform, called Xnode, to improve data synchronization in wireless sensor networks (WSSNs). Recently, the use of the Pulse Per Second (PPS) signal provided by Global Navigation Satellite Systems (GNSS) has become a widely adopted solution for achieving precise timing synchronization [7] [8]. The PPS signal offers high timing accuracy (often within tens of nanoseconds) and long-term stability, which makes it ideal for aligning sensor measurements to a universal time reference, such as Coordinated Universal Time (UTC) [9]. In this context, the present

work presents a developed accelerometer system equipped with GNSS-based synchronization via the PPS signal. The system is designed to provide timestamped data with high temporal precision, allowing integration with other PPS synchronized sensors, such as an interferometric radar. A dedicated hardware and firmware architecture was developed around a Nucleo STM32 microcontroller, which interfaces with a sigma delta ($\Sigma\Delta$) Analog to Digital Converter (ADC) for simultaneous triaxial data acquisition. To validate the performance of the proposed synchronization method, a controlled experiment was conducted using the MEMS-based accelerometer and an X-Band radar system to detect oscillations of a moving bar. Both systems employ high-precision u-blox F9 GNSS receivers, ensuring reliable PPS and UTC data. The results confirm the efficacy of the developed solution in maintaining precise temporal alignment across heterogeneous measurement platforms, laying the foundation for synchronized SHM networks.

ACCELEROMETER SYSTEM DESIGN

The developed system can be seen in Figure 1, which comprehend: the Solgeo AMS PLUS accelerometer, the AccelBoard which is the acquisition board designed to acquire data from the accelerometer and GPS, a Nucleo Board STM32 microcontroller which hosts the firmware, the GPS Receiver Ublox Module and its Antenna which provides the UTC and the PPS from the GPS, and a computer with the developed MATLAB GUI.

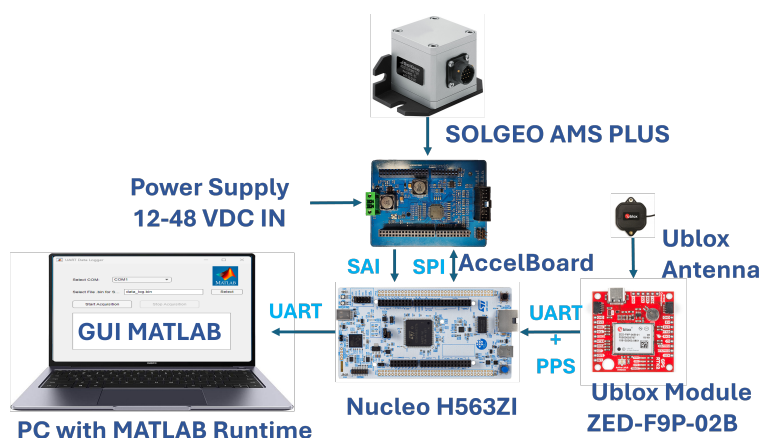


Figure 1. Developed Accelerometer System.

GPS-PPS Synchronization Method

The GPS-PPS synchronization principle is illustrated in Figure 2: the GPS receiver provides, every second, a signal called PPS. PPS is an absolute time source that is highly stable and precise as it is generated by the atomic clocks inside the GPS satellites. Most manufacturers (Trimble, UBlox, Leica, etc.) offer GPS receivers with a PPS precision ranging from 10 to 100 nanoseconds. The logic unit acquires the UTC time from the GPS receiver and converts it in epoch time (the number of seconds elapsed from January 1, 1970 at 00:00:00 UTC to the specified date and time). The UTC epoch has been

updated and synchronized each PPS. The PPS signal is used to reset the internal timer which measure the time digits, e.g. μs . The time stamp t is given by:

$$t = UTC_{base} + N_{PPS} + \delta t. \quad (1)$$

Where UTC_{base} is the epoch of first PPS, N_{PPS} is the number of seconds (number of PPS events) after the first PPS, and δt is the fine accuracy of time expressed in μs . In general, the accuracy of this method is affected by the interrupt latency in capturing the PPS signal, which depends on the type of processor used. Furthermore, the time resolution is determined by the internal timer's precision, which is reset at each PPS signal to prevent the timer from drifting.

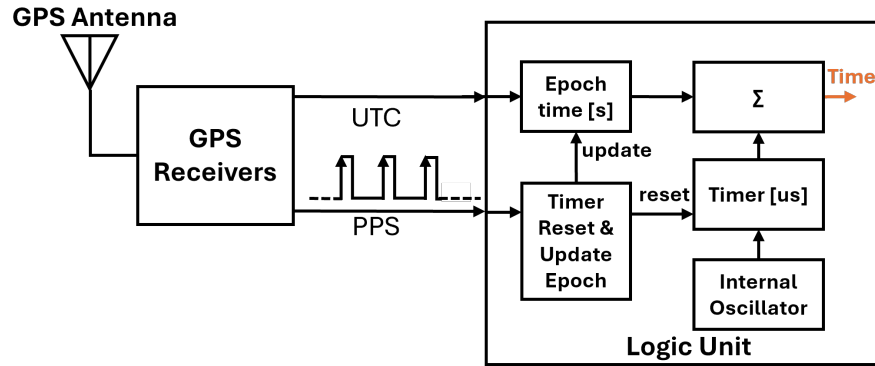


Figure 2. Typical PPS synchronization principle.

Implementation on the micro-controller STM32 NUCLEO Board

The microcontroller (μC) used is a STM32H563, which offers multiple interrupt sources managed by the NVIC (Nested Vectored Interrupt Controller), ensuring low interrupt latency and enables the efficient processing of late-arriving interrupts. Upon power up, the μC configures the ADC and then enables monitoring of the PPS using an EXTI (External Interrupt/Event Controller). This setup allows the μC to capture each PPS from the Ublox Module. Subsequently, the μC acquires the UTC for the first time by decoding the UBX-NAV-TIMEUTC message from the U-Blox F9 module and then enables the internal timer with resolution of $1\mu s$. This approach prevents the loss of first PPS events after acquiring the UTC. Each PPS event triggers an ISR (interrupt Service Routine), which updates the epoch time and resets the internal timer. In addition to handling the PPS interrupt, the μC also must manages the ADC signals through interrupt to associate an accurate timestamps with the incoming data. As well as providing the channels data and the clock, the ADC also generates a data-ready signal to indicate the imminent availability of new data. On the μC , the interface with the ADC is handled via the SAI (Serial Audio Interface), which is suitable for low-frequency (up to tens of kHz) and high-resolution signals. The SAI interface is configured in DMA (Direct Memory Access) triggered by the data-ready signal. Using DMA, the μC can manage other interrupts also during the ADC data acquisition. In this way, the latency of timestamp is reduced. The timestamp is associated to the data-ready signal, which manages an interrupt on the internal timer. The complete algorithm is illustrated in Figure 3.

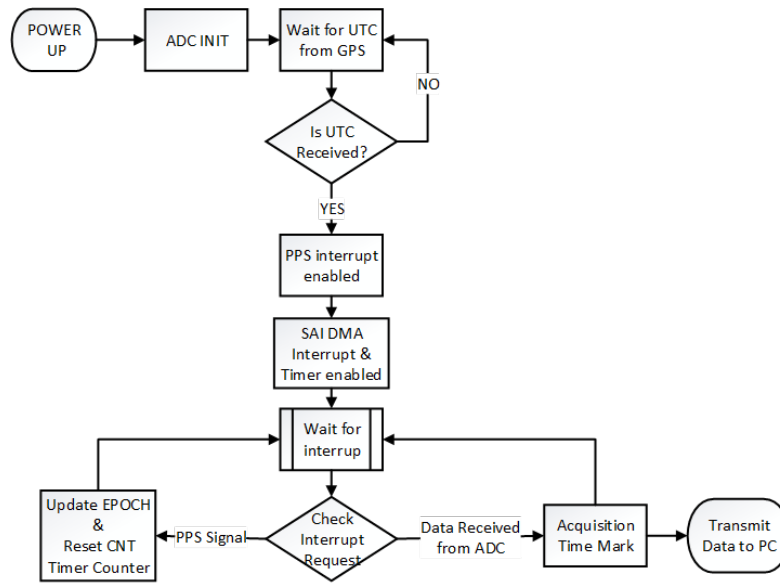


Figure 3. Flow Chart.

Equipment

The accelerometer used was an AMS-PLUS by Solgeo. It is a triaxial accelerometer with $0.7\mu g/\sqrt{Hz}$ of noise density, and a dynamic range larger than 110 dB. This accelerometer is particularly suitable to be used with an interferometric-radar, since it offers an accuracy on displacement (by integrating twice the acceleration) similar or better to the radar. Three channels of the accelerometer have been acquired by the AccelBoard (Figure 1). This board was designed, based on a high resolution $\Sigma\Delta$ ADC. As before explained, the AccelBoard has been connected to the μC which associates the PPS-based timestamp to each ADC data. In particular we used a STM32H563 μC by STMicroelectronics, and a GPS receiver ZED-F9P-02B by Ublox.

EXPERIMENTS AND RESULTS

To validate the developed system a comparison with other PPS-timestamped instruments was made. In particular, we used an X-Band Radar, which was developed to provide a PPS synchronized timestamps. The radar acquires data at a Pulse Repetition Frequency (PRF) of 13.514 kHz, while the accelerometer operates at 1 kHz. Figure 4 shows a schematic representation of the experimental setup of the controlled scenario, which was arranged in a garden at the University of Florence. A corner reflector (CR) was placed on a metallic bar, which was bound to the lower end. The CR was located at 15.5 m away from the position of the radar. On the same metallic bar was installed also the accelerometer, positioned 40 cm lower than the CR position. After the measurement starts, the metal bar, previously held under tension, is released and begins to oscillate.

The synchronization between the two sensors has been verified by comparing the difference between consecutive time stamps. The results are shown in Figure 5. In Figure 5 the average Pulse Repetition Time (PRT) has been subtracted to spotlight the synchrono-

nization event. The peaks in Figure 5 corresponds to the PPS event. Indeed the δt of Equation 1 accumulates latency due to accuracy of internal clock. This cumulative latency is represented by those peaks, since the δt has been reset each PPS. Moreover, there might be an additional delay due to reset operation, which is at maximum of a few of μ seconds. In Figure 5, it can be observed that both systems are resynchronized simultaneously upon receiving the PPS signal. In fact the peaks related to PPS occurring at the same time. The difference in time is related to the different internal clock accuracy and resynchronization procedure. The accelerometer takes about $20 \mu s$ more than the radar each PPS.

Once the synchronization of the two systems has been analyzed, we proceed with the estimation of the displacement. Since the radar measures the displacement of CR, the signal of accelerometer has been retrieved by double time-integration. After each integration, the resulting signal was digital filtered with a Butterworth band-pass filter between 1 Hz and 500 Hz. To compare the displacements measured by both sensors, the displacement retrieved by the accelerometer was linear interpolated on the radar's acquisitions time-vector which acquires at about 13 kHz while the accelerometer system at 1 kHz. As illustrated in Figure 6 it is possible to observe the typical damped oscillating trend. From the zoomed figure on the right side, we can see also how the two trends are in phase, without any shift. After interpolation on a unique time vector, the root mean square deviation between the two sensors was calculated, resulting in 3.1 mm. To obtain this grade of estimation of the displacements, two compensations were made. The first compensation concerns the accelerometer coordinate system. During the oscillation of the pole, there is an effect of rotation on the accelerometer measurement. While the radar measures the displacement along the horizontal plane, the accelerometer measures along its coordinate system. We have to rotate this system onto the horizontal plane. It is possible to estimate this rotation by using the projection of gravity on the accelerometer system. The other compensation regards the difference in altitude between the accelerometer and the CR.

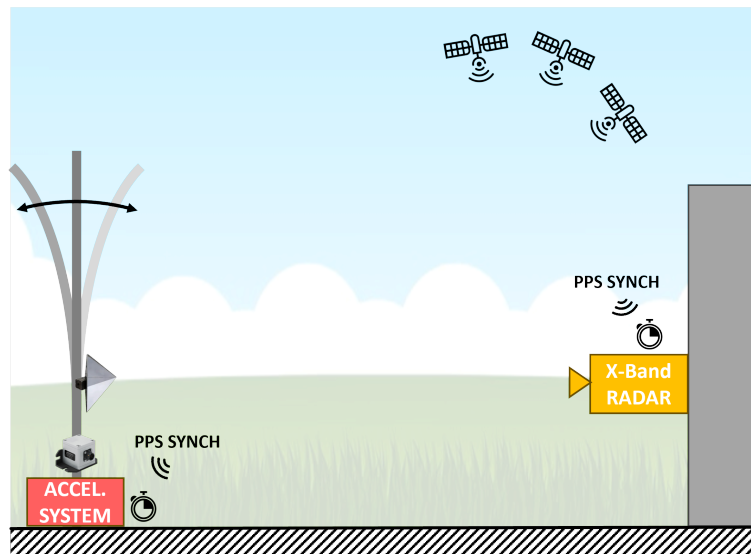


Figure 4. Measurement setup.

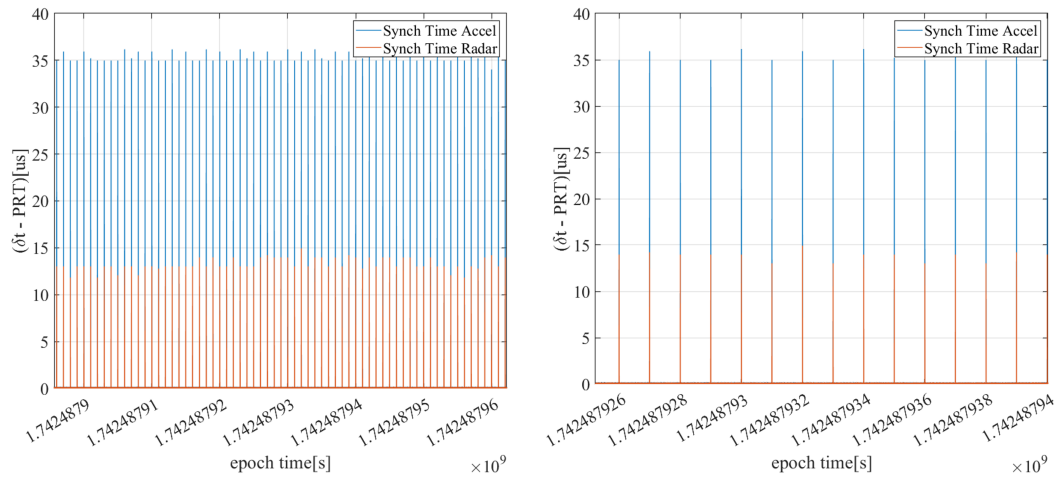


Figure 5. Synchronization Comparison.

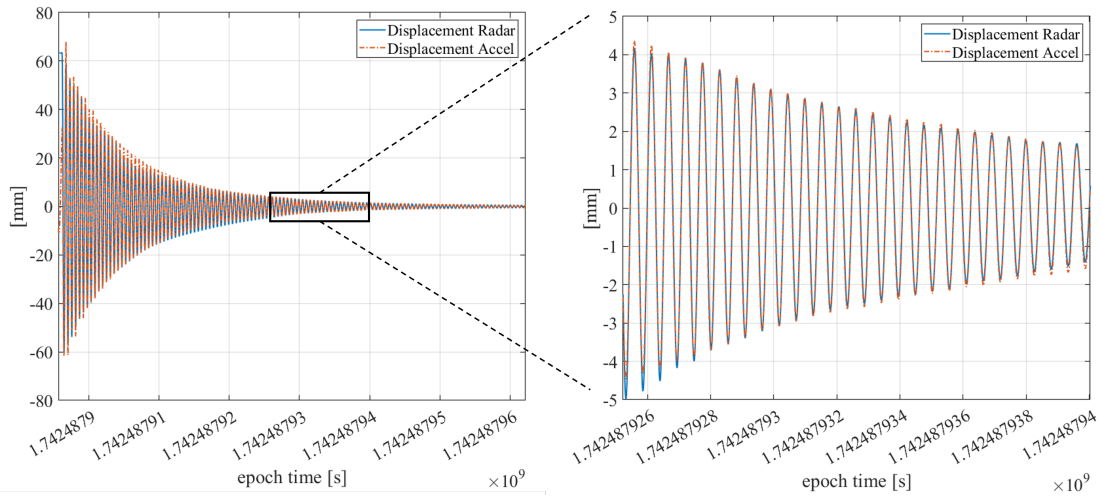


Figure 6. Displacement Comparison: on the left the displacement in whole measurement, on the right a zoom corresponding to the black rectangle.

CONCLUDING REMARKS

In this work, a direct comparison is carried out between the accelerometer and the radar for structural dynamic monitoring. The sensors were simultaneously tested to compare the performance of the systems, in terms of accuracy of displacement estimation and synchronization, for the dynamic monitoring of civil structures such as buildings and bridges. The measurement presented in a controlled scenario, using an oscillating bar, demonstrates the alignment of the displacements measured by two independent sensors, synchronized with the described GPS-PPS synchronization method. The synchronization with the PPS was confirmed, verifying the synchronization events at the same time. The results of the displacements demonstrate the great potential of the synchronization of multiple sensors for structural dynamic monitoring. This study could be the starting point for more advanced analyses and techniques.

ACKNOWLEDGMENT

This research activity has been partially funded by Huawei Technologies, Sweden AB in the framework of a scientific cooperation with the Department of Information Engineering of the University of Florence.

REFERENCES

1. Zhu, L., Y. Fu, R. Chow, B. F. Spencer, J. W. Park, and K. Mechitov. "Development of a High-Sensitivity Wireless Accelerometer for Structural Health Monitoring," 18(1):262, ISSN 1424-8220, doi:10.3390/s18010262, number: 1 Publisher: Multidisciplinary Digital Publishing Institute.
2. Beni, A., L. Miccinesi, L. Pagnini, A. Cioncolini, J. Shan, and M. Pieraccini. "Interferometric Radars for Bridge Monitoring: Comparison among X-Bands, Ku-Bands, and W-Bands," 16(17):3323, ISSN 2072-4292, doi:10.3390/rs16173323, number: 17 Publisher: Multidisciplinary Digital Publishing Institute.
3. Feng, D. and M. Q. Feng. "Computer vision for SHM of civil infrastructure: From dynamic response measurement to damage detection – A review," 156:105–117, ISSN 0141-0296, doi: 10.1016/j.engstruct.2017.11.018.
4. Falletti, E., D. Margaria, G. Marucco, B. Motella, M. Nicola, and M. Pini. "Synchronization of Critical Infrastructures Dependent Upon GNSS: Current Vulnerabilities and Protection Provided by New Signals," 13(3):2118–2129, ISSN 1937-9234, doi:10.1109/JSYST.2018.2883752.
5. Margaria, D. and A. Vesco. "Trusted GNSS-Based Time Synchronization for Industry 4.0 Applications," 11(18):8288, ISSN 2076-3417, doi:10.3390/app11188288, number: 18 Publisher: Multidisciplinary Digital Publishing Institute.
6. Veluthedath Shajihan, S. A., R. Chow, K. Mechitov, Y. Fu, T. Hoang, and B. F. Spencer. "Development of Synchronized High-Sensitivity Wireless Accelerometer for Structural Health Monitoring," 20(15):4169, ISSN 1424-8220, doi:10.3390/s20154169, number: 15 Publisher: Multidisciplinary Digital Publishing Institute.
7. Le Cam, V., A. Bouche, and D. Pallier. "Wireless sensors synchronization: An accurate and deterministic GPS-based algorithm," vol. 1, pp. 1346–1354, doi:10.12783/shm2017/14006.
8. Giammarini, M., M. Pieralisi, D. Isidori, E. Concettoni, C. Cristalli, and M. Fioravanti. "Real-time synchronization of wireless sensor network by 1-PPS signal," in *Smart Sensors, Actuators, and MEMS VII; and Cyber Physical Systems*, SPIE, vol. 9517, pp. 300–309, doi: 10.1117/12.2179479.
9. Salazar-Lopez, J. R., J. R. Millan-Almaraz, J. R. Gaxiola-Camacho, G. E. Vazquez-Becerra, and J. M. Leal-Graciano. "GPS-Based Network Synchronization of Wireless Sensors for Extracting Propagation of Disturbance on Structural Systems," 24(1):199, ISSN 1424-8220, doi: 10.3390/s24010199, number: 1 Publisher: Multidisciplinary Digital Publishing Institute.